



ELSEVIER

Thermochimica Acta 318 (1998) 213–220

thermochimica
acta

Simulation of the sintering behavior of a ceramic green body using advanced thermokinetic analysis

J. Opfermann*, J. Blumm, W.-D. Emmerich

NETZSCH-Gerätebau GmbH, Wittelsbacherstr. 42, D-95100 Selb, Bavaria, Germany

Received 17 October 1997; accepted 26 January 1998

Abstract

The sintering behavior of an alumina green body was measured at three different heating rates using a high-temperature pushrod dilatometer. The measurement results were evaluated with a complex thermokinetic analysis program. Using the calculated kinetic parameters, predictions were made for the behavior under rate controlled sintering conditions. The resulting temperature profiles were compared with the results of actual rate controlled sintering measurements. Good agreement was found between the experimental data and the thermokinetic prediction. © 1998 Elsevier Science B.V.

Keywords: Alumina; Sintering; Kinetics; Rate controlled thermal analysis; Simulations

1. Introduction

Ceramic materials can be produced in many different ways. One of the most common methods is mixing a fine ceramic powder with an organic binder. From this mixture, a green body with a specific geometry can be shaped, for example, by means of cold-isostatic pressing. In the subsequent production process, the organic binder is removed from the shaped green body, e.g. by thermal treatment. Further, the green body is sintered at elevated temperatures to produce a dense ceramic part. Many properties of the final ceramic part, such as densification or porosity, are strongly dependent on the conditions under which the ceramic green body is sintered. One of the most important parameters is the temperature program during sintering, especially the heating rate.

Pushrod dilatometers are frequently used to examine the sintering behavior of ceramic materials. Here, the thermal expansion or shrinkage of a sample is measured as a function of temperature or time at constant heating or cooling rates. The method of dilatometry as well as the fundamental principles are explained in detail by Speyer [1] and Valentich [2]. Applications of dilatometry in the field of ceramics have been described by Kaisersberger and Kelly [3]. Using dilatometers, it is possible to measure the rates of shrinkage under different conditions (i.e. different heating rates). Through various examinations, it was found that, for many ceramic materials, the rate of shrinkage and densification are higher if a low rate of shrinkage is achieved during the sintering process. This can be realized in most cases by using a low heating rate. On the other hand, the goal for industrial applications is to use fast temperature programs for sintering processes. One possibility for achieving a temperature profile with both, a fast

*Corresponding author. Tel.: +49 9287 88141; fax: +49 9287 88144; e-mail: ngb@netzsch.com

heating rate – when no shrinkage occurs – and a low rate of shrinkage during the sintering process is the use of a rate controlled sintering dilatometer. Here, one of the standard operating principles of a pushrod dilatometer is altered in such a way that constant rates of shrinkage can be detected. This is accomplished by modifying the temperature program (heating rate) within the sintering range. The method of rate controlled sintering has been presented elsewhere in more detail, e.g. Palmour III [4–6] and Semar et al. [7].

Using rate controlled sintering (RCS), it is possible to measure temperature profiles for sintering processes and to examine the dependence between shrinkage rate and densification. One problem with this method is that a new measurement must be carried out for each sintering rate. This can be a very time-consuming procedure, especially if the shrinkage is to be examined under complex temperature programs, with heating, cooling and isothermal segments. The approach of this work was to measure the sintering behavior of a ceramic green body at several different constant heating rates. The results were analyzed using an advanced thermokinetic software package [11]. The basic concepts of the software package, as well as other applications have been described by Kaisersberger and Opfermann [9] and Opfermann et al. [8,10]. After analysis of the shrinkage curves with the thermokinetic software and evaluation of the kinetic parameters, it was possible to predict the behavior under rate-controlled sintering conditions. Therefore, the temperature profile for a predefined sintering rate was determined without carrying out further measurements. To prove the capability of this approach, comparisons were made between actual RCS measurements and the predictions.

2. Material

The sample material was an alumina green body with $\approx 80\%$ alumina content. The content of organic binder was $<3\%$. The remainder of the material was made up of sintering additives which reduce the sintering temperature and modify the sintering behavior of the samples.

The samples examined were cylinders with diameters of 4 mm. The length of the samples, measured at constant heating rates, was ≈ 15 mm. Samples,

15.7 mm long, were prepared for the RCS measurements. The same sample lengths were used for each RCS measurement, thus reducing additional influences and simplifying the subsequent comparison of the results.

3. Experimental

The sintering behavior was measured using a Netzsch model 402C single-pushrod dilatometer. The system was equipped with an SiC furnace, allowing measurements to be carried out between room temperature and 1550°C . An alumina sample holder and pushrod were employed for the measurements. The measurement system is shown in detail in Fig. 1. All examinations were performed in static-air atmosphere. Thin (0.5 mm) alumina disks were positioned between the sample holder, sample and pushrod to protect the measurement system from adhesion with the sample. Measurements were carried out from room temperature to $\approx 1425^\circ\text{C}$ at three different heating rates: 5, 10 and 20 K/min. To correct the influences of the measurement system, calibration measurements were carried out using a sapphire standard. The calibration runs were, of course, carried out under the same conditions as those used for the samples.

The RCS measurements were carried out between room temperature and $\approx 1400^\circ\text{C}$ at a nominal heating rate of 10 K/min. Measurements were performed at two different threshold values for the sintering rate. The RCS software was set to the start/stop mode, where heating was stopped when the predefined sintering rate was exceeded and restarted when the sintering rate fell below the given value. Therefore, the average shrinkage rate measured during RCS was somewhat higher ($\approx 4\%$) than the predefined values. The 20 $\mu\text{m}/\text{min}$ threshold value yielded an average shrinkage rate of 20.9 $\mu\text{m}/\text{min}$ (0.133%/min). At a threshold value of 30 $\mu\text{m}/\text{min}$, the resulting average shrinkage rate was 31.1 $\mu\text{m}/\text{min}$ (0.198%/min). The RCS measurements were corrected using a sample holder correction.

4. Results and discussion

The linear shrinkage of the alumina green body at constant heating rates is depicted in Fig. 2 over a

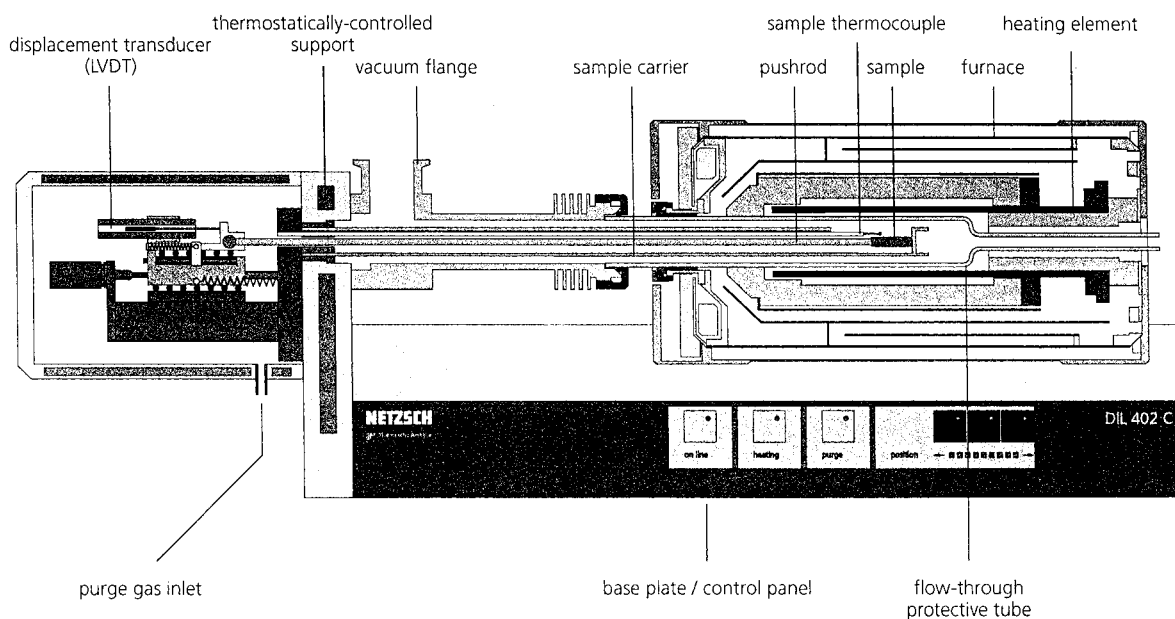


Fig. 1. Schematic diagram of the dilatometer used for the measurements.

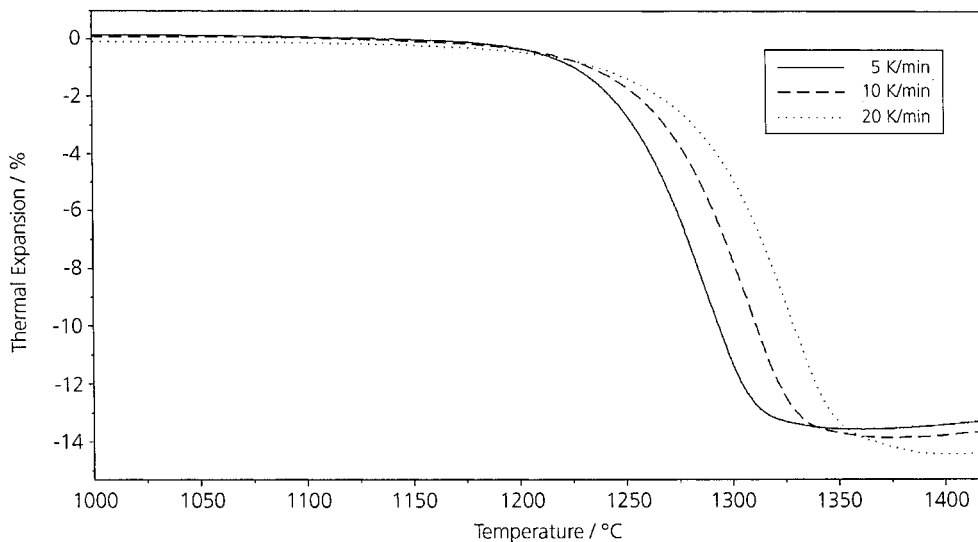


Fig. 2. Linear shrinkage of the alumina green body during sintering at three different heating rates: (solid line), 5; (dashed line), 10; and (dotted line) 20 K/min.

1000–1420°C range. The solid line represents the measurement at a heating rate of 5 K/min, the dashed line – at 10 K/min and the dotted line – at 20 K/min. The beginning of sintering was detected at ≈1200°C for all three heating rates. As can be seen, the range of

sintering expands with increasing heating rate. For the 5 K/min measurement, sintering is complete at ≈1350°C, while for the 20 K/min, it is complete at ≈1400°C. Furthermore, it can be seen that higher shrinkage rates were detected for higher heating rates.

This behavior is unusual for alumina samples and is most probably caused by the sintering additives. Therefore, the advantages usually connected with rate controlled sintering, e.g. higher densification, are not valid for this sample material. This phenomenon causes no problems for the thermokinetic analysis and the predictions using the given software package.

In general, kinetic analysis is carried out in order to clarify the mechanism of the reaction under investigation. In addition to this scientific aspect, of equal importance is the technical aspect, i.e. the use of kinetic analysis as an efficient tool for the description of the observed processes without a mechanistic interpretation of the results. In the end, the drastic reduction of data achieved with kinetic analysis allows prediction of the reaction profile, even for temperature programs not included in the measurement [11,12]. To ensure that such predictions have a high level of confidence, a sufficient portion of the three-dimensional reaction field signal=signal (time, temperature) must be recorded with the base measurement [13] since from a statistical view, the predictions within the recorded reaction field exhibit, a priori, a high level of confidence with a good fit of the base measurement through kinetic analysis. Outside the recorded reaction field the level of confidence generally decreases.

In view of the foregoing consideration, the kinetic analysis must achieve the following: a fit of measurements with different temperature profiles by means of a common kinetic model.

Model-free methods for determining the activation energy are helpful in the development of the model. Fig. 3 shows a corresponding Friedmann analysis

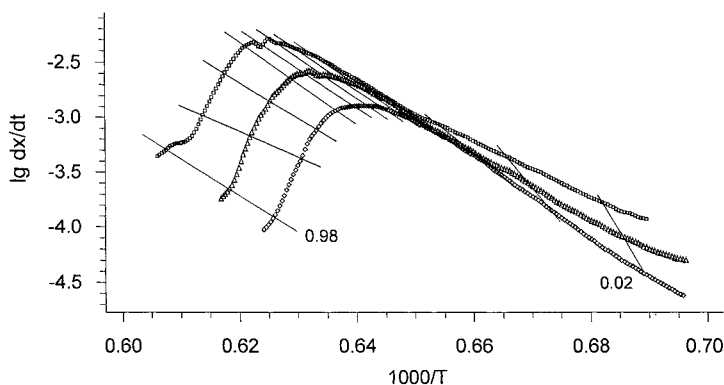
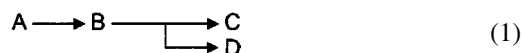


Fig. 3. Friedman analysis of the measurements at different heating rates.

[14]. The figure depicts the differentiated expansion vs. the reciprocal temperature. One peak is observed in the differentiated expansion curve. A possible cause of this could be competing reactions during the sintering process. This is confirmed through the fact that there is a relation between the total shrinkage and heating rate in the dilatometer measurements (Fig. 2). Such a fact can even be seen as adequate proof for the existence of appropriate reaction sequences.

Fig. 4 shows an additional result of the Friedman analysis, the activation energy as a function of partial-length change. The curve shows a considerably higher value at the beginning of the sintering process, i.e. at lower partial-length-change values. This indicates the presence of a multiple-step process for which a very high activation energy must be assumed for the first step.

Taking these findings into consideration, a fit was attempted using nonlinear regression with model (1), where the n th-order (F_n) reaction type was used for all steps of the reaction:



It was found that the fit quality is significantly improved if the first step of model 1 is broken down into two consecutive reactions although such a separation is not visually observed. With this expanded model, an excellent fit is possible for all three measurements and the essential characteristic, i.e. the dependence of the total shrinkage on the heating rate, is conveyed correctly (Fig. 5). The parameters are listed in Table 1.

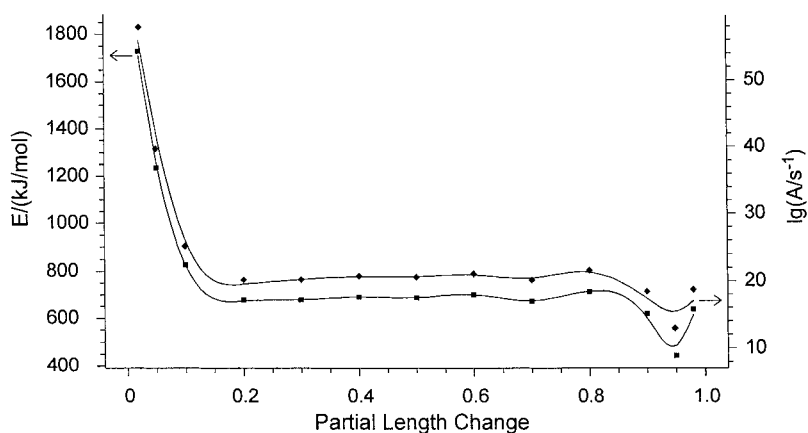


Fig. 4. (■) Activation energy E and (◆) $\lg A$ vs. change in partial length, calculated by the Friedman analysis.

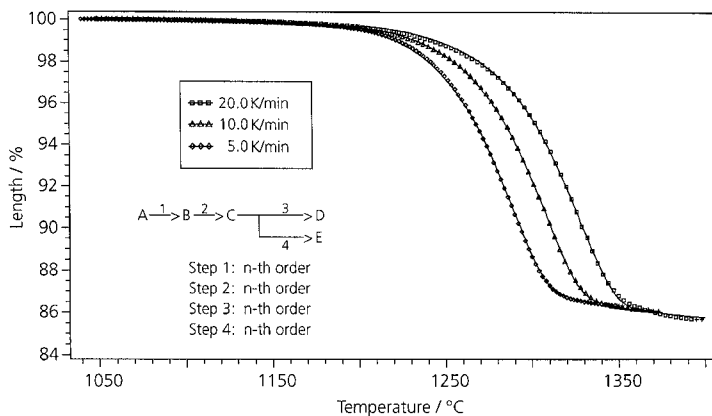
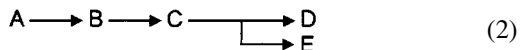


Fig. 5. Kinetic analysis of the measurements at three different heating rates.



The core of the program is the multivariate non-linear regression, which works with a hybrid Marquardt–Levenberg process [15]. The initial values for the iterative computation were taken from the model-free determination of the activation energy. By setting secondary conditions, the solution was limited to a reasonable range. Thus, for example, the parameters Reaction orders 1 and 2 were set as constant values.

It is interesting to note the result that the first two formal reaction steps, which determine the start of sintering with their high activation energy ($E_1, E_2 > 1000$ kJ/mol), contribute only slightly to the total shrinkage ($\approx 4.8\%$). The actual shrinkage is described

by the competing steps, 3 and 4, whose activation energies are considerably lower ($E_3, E_4 < 700$ kJ/mol). This separation of the sintering process into single stages is in agreement with general observations [16].

The results for the rate controlled sintering measurements at the two predefined threshold values 20 (solid lines) and 30 $\mu\text{m}/\text{min}$ (dashed lines) are shown in Fig. 6. It can be seen that, below the sintering range, the temperature profiles as well as the thermal expansion curves are equivalent for the two measurements. Small differences in the expansion behavior can be explained by material inhomogeneities within the two samples. At temperatures above $\approx 1200^\circ\text{C}$, the situation changes. When the shrinkage rate reaches the predefined threshold values, heating is stopped and

Table 1
Kinetic parameters

No.	Parameter ^a	Value
1	$\log A_1/s^{-1}$	40.211
2	$E_1^b/(kJ/mol)$	1149.239
3	Reaction order ^c 1	2.000 const.
4	$\log A_2/s^{-1}$	48.363
5	$E_2^b/(kJ/mol)$	1446.068
6	Reaction order ^c 2	4.000 const.
7	$\log A_3/s^{-1}$	19.506
8	$E_3^b/(kJ/mol)$	664.544
9	Reaction order ^c 3	0.693
10	$\log A_4/s^{-1}$	20.431
11	$E_4^b/(kJ/mol)$	695.228
12	Reaction order ^c 4	0.611
13	Foll. React. ^d 1	3.187E-03
14	Foll. React. ^e 2	1.035E-02
15	Comp. React. ^f 3	4.123E-04
16	Comp. React. ^g 4	0.2734

^a $\log A_n/s^{-1}$ – logarithm of the pre-exponential of reaction step n .

^b $E_n/(kJ/mol)$ – activation energy of reaction step n .

^c Reaction order n – order of reaction of reaction step n .

^d Foll. React. 1 – portion of total shrinkage of consecutive reaction 1.

^e Foll. React. 2 – portion of total shrinkage of consecutive reaction 2.

^f Comp. React. 3 – portion of total shrinkage of competitive reaction 3, if the reaction follows this path completely.

^g Comp. React. 4 – portion of total shrinkage of competitive reaction 3, if the reaction follows this path completely.

restarted after the measured shrinkage rate falls below the threshold value. As a result, the temperature profile is modified such that the shrinkage rate of the samples

is approximately constant. Due to the lower threshold value of the 20 $\mu\text{m}/\text{min}$ measurement (solid line), the resulting average heating rate during sintering is lower, as well. Therefore, the temperature stays at a lower level. On the other hand, it is clear that the sintering time is extended for the lower threshold value.

In Fig. 7, a comparison is made between the rate-controlled sintering measurement at the 20 $\mu\text{m}/\text{min}$ threshold value and a prediction of the thermokinetic software. The actual (measured) shrinkage rate (0.133%/min) was used as an input parameter for the simulation. As can be seen, there is practically no deviation between the measured (circles) and simulated (dashed line) length change. The calculated (solid line) and measured (squares) temperature profiles are also in good agreement. Only in the time range above 210 min, where sintering ends, can small deviations be seen. In most of the sintering range, the deviation between the measured and predicted temperatures is $<6^\circ\text{C}$.

The deviations between measurements and predictions made using the thermokinetic software can be explained, for example, by the following. The rate controlled sintering measurements were carried out in the start/stop mode. This mode causes a temperature program that does not increase uniformly during the sintering process. The kinetic software package, on the other hand, calculates a stepwise constant heating

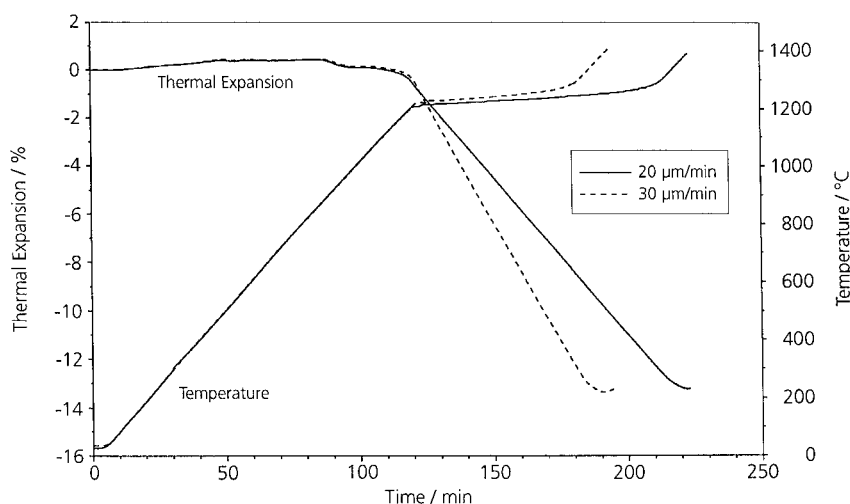


Fig. 6. RCS measurements at predefined threshold values of (solid line) 20 and (dashed line) 30 $\mu\text{m}/\text{min}$.

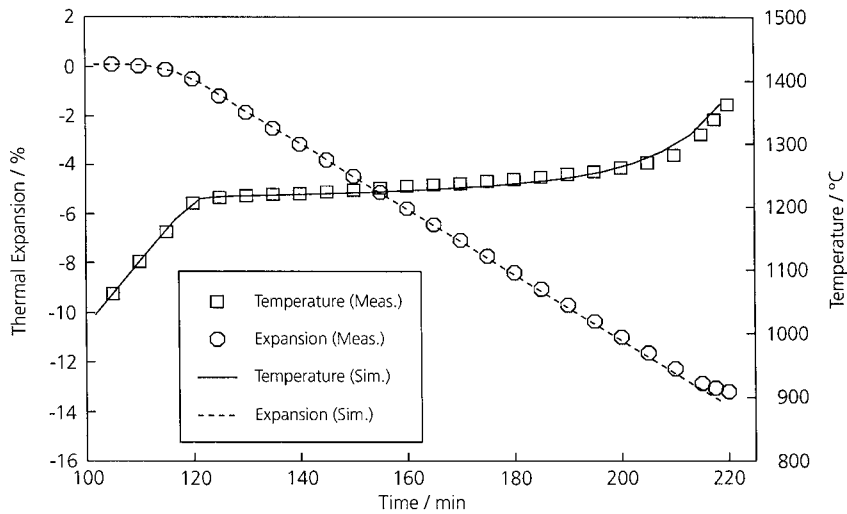


Fig. 7. Comparison of change in length and temperature profile of an actual RCS measurement (threshold value: 20 $\mu\text{m}/\text{min}$) and the kinetic prediction.

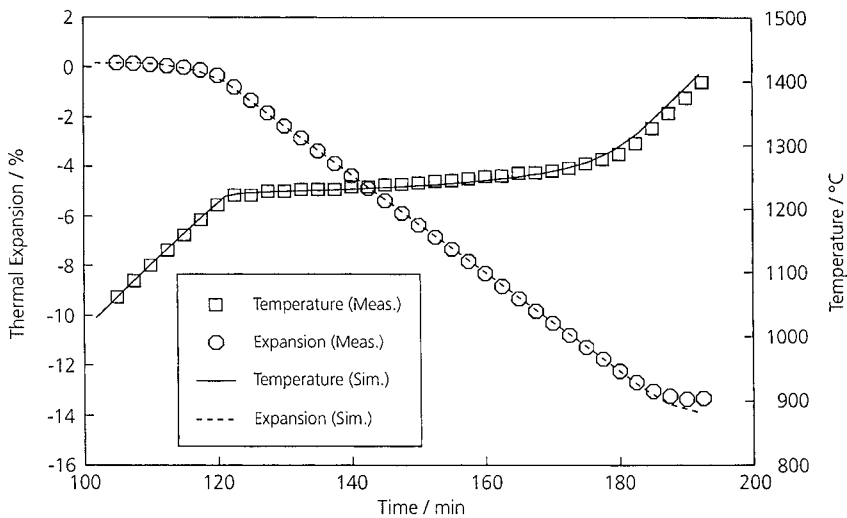


Fig. 8. Comparison of the actual RCS measurement (threshold value: 30 $\mu\text{m}/\text{min}$) and the kinetic prediction.

rate for the sintering range. Therefore, small deviations between the measurement and the prediction can be expected.

The comparison between the rate controlled sintering measurement and the prediction for the 30 $\mu\text{m}/\text{min}$ threshold value is presented in Fig. 8. Here again, only small deviations between the measured (squares) and predicted (solid line) temperature profiles can be seen.

5. Conclusions

An advanced thermokinetic software package was used to analyze the sintering process of an alumina green body. Using the evaluated kinetic model and its parameters, predictions were possible regarding the behavior under rate controlled sintering conditions. Comparisons with actual-rate controlled

sintering measurements prove the reliability of this method.

It is to be expected that the model found requires further refinement, e.g. because reaction steps other than n th-order reactions may prove to be optimal.

References

- [1] R.F. Speyer, Thermal Analysis of Materials, Marcel Dekker Inc., New York, 1994, p. 165.
- [2] J. Valentich, Tube Type Dilatometers, Instrument Society of America, Research Triangle Park, North Carolina, 1980.
- [3] E. Kaisersberger, J. Kelly, Int. J. Thermophys. 10(2) (1989) 505.
- [4] H. Palmour III, T.M. Hare, in: G.C. Kuczynski, D.P. Uskokovic, H. Palmour III et al. (Eds.): Sintering '85, Plenum Press, New York, 1987, p. 17.
- [5] H. Palmour III, M.L. Kuckabee, T.M. Hare T, in: M.M. Ristic (Ed.), Sintering – New Developments, Elsevier, Amsterdam, 1979, p. 46.
- [6] H. Palmour III, Ceram. Eng. Sci. Proc. 7 (11–12) (1986) 1203.
- [7] W. Semar, W. Pannhorst, T.M. Hare, H. Palmour III, , Glastechnische Berichte 62(2) (1989) 74.
- [8] J. Opfermann, G. Wilke, W. Ludwig, E. Kaisersberger, M. Gebhardt, S. Hagen, in: Thermische Analysenverfahren in Industrie und Forschung (VI. Herbstschule), Friedrich-Schiller-Universität Jena, 1991, pp. 51–79.
- [9] E. Kaisersberger, J. Opfermann, Laborpraxis 4 (1992) 360.
- [10] J. Opfermann, F. Giblin, J. Mayer, E. Kaisersberger, American Laboratory (1995) 34.
- [11] J. Opfermann, Thermochim. Acta, in preparation.
- [12] J. Opfermann, E. Kaisersberger, Thermochim. Acta 203 (1992) 167.
- [13] J. Opfermann, W. Hädrich, Thermochim. Acta 263 (1995) 29.
- [14] H.L. Friedman, J. Polym. Sci. C6 (1965) 175.
- [15] J. Opfermann, Rechentechnik/Datenverarbeitung 23 (1985) 26.
- [16] H. Salmang, H. Scholze, Keramik, Teil 1 – Allgemeine Grundlagen und wichtige Eigenschaften, Springer-Verlag, Berlin, Heidelberg, New York, 1982, p. 165.